Non-Contact Breathing Detection Using Passive Radar

Wenda Li, Bo Tan and Robert J. Piechocki
Department of Electrical and Electronic Engineering
University of Bristol
Bristol, UK
wenda.li, b.tan, r.j.piechocki@bristol.ac.uk

***Abstract*—Non-contact breathing monitoring systems are very attractive for a range of e-Healthcare applications. This paper proposes a passive radar based system for measuring human breathing rate. A novel signal processing method is introduced to extract breathing rate based on micro Doppler derived from cross ambiguity function (CAF). The passive radar system is built within a software defined radio (SDR) platform. The proposed system uses opportunistically energy harvesting transmitter as an illumination signal. Passive detection is compared and verified using the ground truth from clinical chest belt respiration detector. Two experiments have been conducted to show the feasibility of passive detection system in the line of sight and also through-wall conditions. We conclude that a low frequency narrow band signal with non-contact passive detection can offer a realistic alternative to UWB based radars for future e-Healthcare passive sensing applications.**

I. Introduction

Respiration is one of the most informative vital signs since it contains important information which includes the cognitive state, sleep pattern, and cardiovascular condition. It may be useful in prevention of potential threats such as sudden heart attacks and a risk of falling. Typically, a complete respiration cycle is defined by a pulse accompanied with inhalation (inspiration) and exhalation (expiration) states as described in [1]. The chest wall or abdomen displacement information during inhalation and exhalation can potentially indicate the types of breathing and can be used to identify breathing patterns. The traditional respiration measurement method is to use some contact sensors or chest belt to measure the dynamic movement of chest wall or abdomen [2]. Non-contact sensing of breathing without attachment to the patients skin can provide an attractive and alternative means to e-Healthcare applications, and already been considered in patient monitoring in either clinical or residential scenarios.

Studies have shown the feasibility of non-contact breathing detection with both high accuracy and low complexity. Using non-contact ultrasonic sensor to detect human respiratory motion is developed in [3] by measuring the frequency shift of the reflected ultrasound caused by the velocity difference during respiration cycle. Narrow-band radar developed in [4] and ultra-wide-band (UWB) radar technique developed in [5], [6], [7] are used to detect displacement difference caused by the chest movement. Unlike the narrow-band signal, UWB radar delivers a fine range resolution on a scale from a few centimeters to one centimeter. However, all above methods are require active radar (radar like) system: which requires one or more specifically designed transmitters with controlled waveform, increasing the cost and the complexity of the system.

In this paper we advocate a non-contact detection system that is source-free by using an illumination signal opportunistically. The principle of the passive radar system is to capture the time and frequency difference between the source and reflected signal, which represents the distance and the velocity status of the object. In this work, we choose the Energy Harvesting technology (EH) as the illumination signal due to its relatively high transmission power and continuous signal nature. Such devices become a comon place in many e-Heath IoT applications. The EH device used in this work transmits a narrow-band DSSS modulated signal with 26 MHz bandwidth in the sub 1 GHz ISM band. Due to the limitation of the bandwidth, the coarse range information cannot be used anole for respiration identification, therefore, we only consider the Doppler information.

The state of the art in passive radar in indoor scenarios is discussed in [8] and [9] which use WiFi signal as the illumination signal and successfully capture the small Doppler shift caused by the hand and body movements. However, both works have not demonstrated the respiration detection, since slow and tiny chest movements generate only micro and inconspicuous Doppler shift that can not be easily extracted from the reflected signal. To the best of our knowledge, this is the first work investigating the feasibility of the non-contact breathing detection with narrow band passive radar. Additiopnally we propose a micro Doppler extraction method based on the CAF mapping. The system is implemented and verified on the Universal Software Radio Peripheral (USRP) running with LabVIEW.

The rest of this paper is organized as follow: Section II describes the signal processing of proposed passive system including, optimum batching process for CAF mapping and the micro Doppler extraction. Section III describes the architecture of proposed passive system and demonstrates the concept of obtaining breathing, followed with experiments in both line of sight and through wall illumination conditions. Section IV gives the conclusion and the future work.

II. Passive Radar Signal Processing and Micro Doppler Extraction

A. Batching Process and CAF mapping

The traditional way to extract range and Doppler information is to process the received reference and surveillance signal by CAF mapping. In this section, a mathematical definition of the batching CAF process is derived for the passive system, starting form CAF mapping equation as (1):

$$CAF(\tau, f_d) = \int_0^T S_{sur}(t) S^*_{ref}(t-\tau) e^{j\phi(t)} dt \tag{1}$$

where $s_{ref}(t)$ is the direct reference signal from the illuminator, $s_{sur}(t)$ is the received signal from the surveillance area, f_d is the Doppler shift, ϕ is the phase and τ is the propagation delay. The reference signal can be divided into several segments that contain same length T_B of data [10], and can be written as (2):

$$s_{ref}(t) = \sum_{k=0}^{n_b-1} s^k_{ref}(t - kT_B) \tag{2}$$

where n_b is the number of segments, defined as (3):

$$n_B = \left\lfloor \frac{2 * v_{max} * f_c * T_B}{c} \right\rfloor \tag{3}$$

Where $\lfloor . \rfloor$ indicates the maximum integer value that is smaller than the argument, v_{max} is the maximum target velocity, c is the speed of light and f_c is the carrier frequency of the signal. The factor 2 is used to account the Doppler shift in both positive and negative domain. Substituting (2) into (1), the CAF mapping can be written as (4):

$$CAF(\tau, f_d) = \sum_{k=0}^{n_b-1} \int_0^T S^k_{sur}(t) {S^k_{ref}}^*(t - kT_B - \tau) e^{j\phi(t)} dt \tag{4}$$

where the $s^i_{sur}(t)$ can be divided as same equation (2) from the $s_{sur}(t)$. T is the integration time in the time domain of received signal for the batching process. The main steps of this process can be presented schematically in Fig. 1.

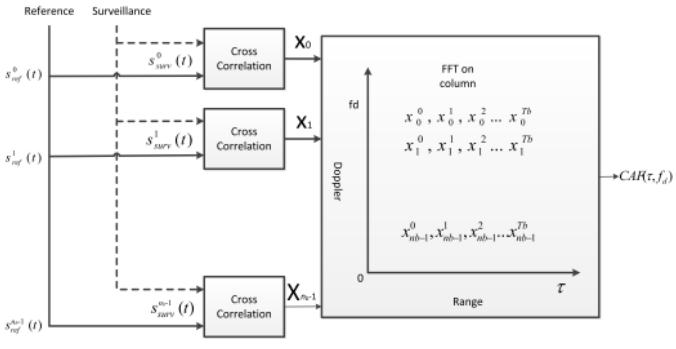

Fig. 1. Batching process for CAF mapping.

B. Micro Doppler Extraction

The challenge for breathing detection in a passive radar system is the micro Doppler extraction. The Doppler resolution Δf is inversely proportional to the integration time, $\Delta f = \frac{1}{T}$. Theoretically, increasing the integration time can provide sufficient Doppler resolution for the micro Doppler shift. However, the Doppler shift is assumed to be constant during the period of integration, which presents a limitation on the duration of the signal that can be integrated. Therefore, the movement should be a comparable constant in both direction and velocity, so that it can be recognized by the traditional CAF mapping. In our case, a complete breathing motion including inhalation, exhalation and unexpected body gestures. Increasing the integration time will output both positive and negative Doppler shifts in one time or range bin on CAF mapping and mislead the further analysis. Therefore, it is not practical to increase the integration time for the breath detection. As a result, the Doppler resolution is not sufficient for small Doppler extraction purpose. To extend the ability of recognising the tiny Doppler shift, the new micro Doppler extraction is proposed based on the CAF mapping (equation (4)).

Let's start with the position of the maximum of time-frequency distribution, we can pick a column containing the Doppler peak from a single CAF mapping, then combine a number of peaks to form a spectrogram $D(f_d, n)$ - the method is described following (5):

$$D(f_d, n) = \sum_{n=0}^{k-1} arg_{f_d} \{ maxCAF_n(\tau, f_d) \} \tag{5}$$

where CAF_n represents one single CAF mapping, k is the total number of recorded CAF mapping in a spectrogram, $arg_{f_d}\{.\}$ donates the column with maximum peak on the Doppler axis. The main step of this process is shown in Fig. 2.

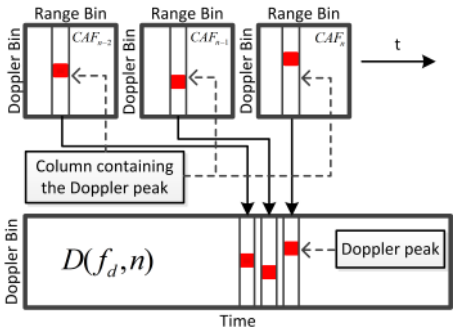

Fig. 2. Process for Spectrogram

Due to the limitation of the integration time, the Doppler shift caused by the chest movement is not sufficient for jumping to another Doppler bin in the CAF mapping. However, we observe that the shape of the Doppler peak relates to the reflected signal, even a tiny motion can deduce a slight difference. Fig. 3 presents two adjacent Doppler pulses from

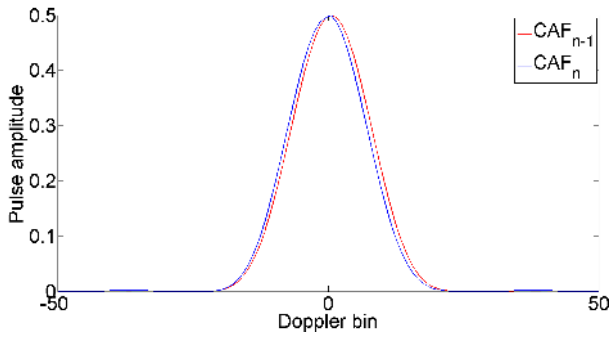

Fig. 3. Two adjacent Doppler pulses.

CAF_n and CAF_{n-1}, both measured from a breathing cycle. As can be seen both peak occupies in the same Doppler bin that outputs same Doppler shift. However, there is slight shape difference between two pulses. This difference is caused by the chest movement. By measuring the difference of each Doppler peak, it is possible to extract the hidden micro Doppler information that is linked with breathing [11]. To demonstrate this concept, we introduce a parameter $\Psi(n)$ as the metric of the shape of Doppler peak.

We calculate shape difference as the metric which can be deduced by comparing the amplitude value in both positive and negative Doppler domains. The volume of $\Psi(n)$ depends on the peak's tendency in the CAF mapping. To distinguish the positive and negative Doppler shifts, we apply different sign to the positive and negative domain. Let j be the size of one column in $D(f_d, n)$ and i be the index of column. Then the intensity of $\Psi(n)$ can be estimated by the instantaneous extraction as (6):

$$\Psi(n) = \sum_{n=0}^{k-1} \sum_{i=0}^{j-1} f_d^i(n) * \left\lceil (\frac{j}{2} - i) \right\rceil \tag{6}$$

where $\lceil . \rceil$ represents the sign of the argument which is used to compensate the positive and negative domain. The shifted Doppler map $D(f_d, n)$ can be also seen as (7):

$$D(f_d, n) = D(f_D, n) + D(f_{mD}, n) \tag{7}$$

where $D(f_D, n)$ denotes the major Doppler shift in different Doppler bin (normally caused by large movement), $D(f_{mD}, n)$ is the micro Doppler (normally caused by the relative small movement). Assume the target is in a stationary state so that the major Doppler shift remains in the 0 Doppler bin, the $D(f_D, n)$ can be be neglected, therefore $\Psi(n)$ can be written as (8):

$$\Psi(n) = \sum_{n=0}^{k-1} \sum_{i=0}^{j-1} f_{mD}^i(n) * \left\lceil (\frac{j}{2} - i) \right\rceil \tag{8}$$

The effect of $\Psi(n)$ in equation (8) which present the respiration is demonstrated in the section III B (shown in Fig. 6).

III. System Demonstration & Experiments

In this section we present the whole proposed passive system, then we demonstrate the concept of obtaining breathing from micro Doppler through the passive system. Two experiments were carried out to verify the proposed passive principle for breathing detection. Two different layouts had been used to investigate the feasibility of the passive system in different scenarios. The experiments layout and results are described in detail below.

A. Architecture of the System

A passive system is based on two NI USRP-2920 [12] platform that has been built for real-time signal acquisition. Each NI USRP 2920 is fitted with a WBX daughterboard which has a frequency range of 50-2200 MHz, the architecture includes a Xilinx FPGA (3A-DSP 3400) and a 100 MS/s,14-bit ADC and a Gigabit Ethernet connectivity to stream data to the host computer for signal processing and results display. The computational unit implements the main signal processing with LabVIEW and running with a laptop. With the batching process design and low complexity of micro Doppler extraction, this system is able to record breathing signal in real-time. Fig. 4 shows the block diagram of the proposed passive system.

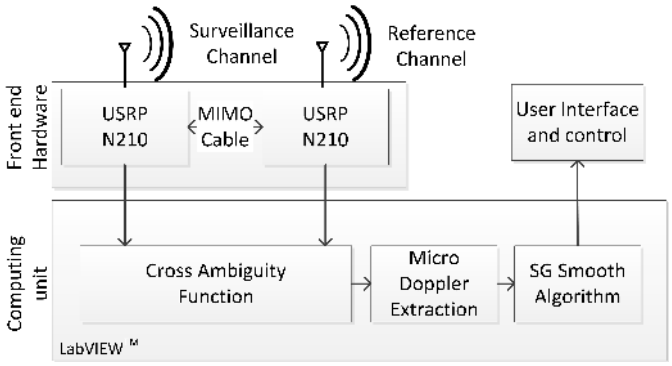

Fig. 4. Block diagram of the proposed passive system

B. Breathing rate extraction from micro Doppler

For this demonstration, a participant is positioned 0.4m away from the antennas where the surveillance antenna is aligned with the chest to capture the Doppler effect. The EH transmitter is 1.5 meters away from the person. The reference antenna is pointing to the EH transmitter while the surveillance antenna is pointing towards the person. The experiment layout is shown in Fig. 5.

Typically, normal breathing rate of an adult ranges from 12-20 breaths/min [13]. Fig. 6(a) shows a 30 second breathing signal by depicting the max Doppler peak from the traditional CAF mapping (by using equation (5)), as it can be seen the breathing signal is unclear and provides insufficient Doppler information. Since the amplitude and frequency of chest movement are not adequate for a Doppler peak jump more then one Doppler bin. The proposed Doppler extraction (by using equation (8)) has been applied to the Fig. 6(a) and

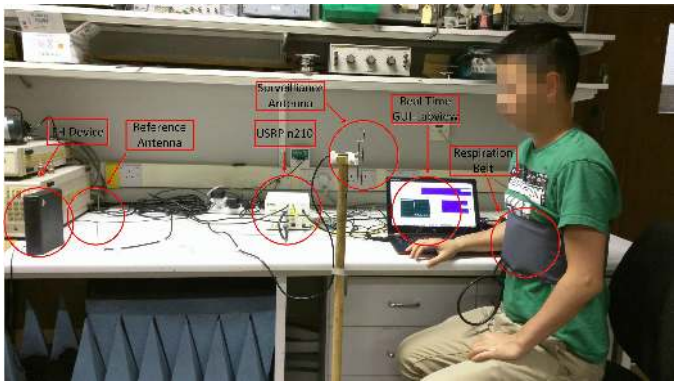

Fig. 5. Experiment layout: participant is facing to the surveillance antenna.

the result is shown in Fig. 6(b). This method successfully extracts the breathing signal from the CAF mapping and shows 6 respiration cycles in 30s. Although the breathing period is clear and is able to be distinguished, the waveform is noisy and it is difficult to accurately determine the inhalation and exhalation state within one breathing cycle. Fig. 6(c) shows the breathing signal when Savitzky-Golay filter is applied, and it clearly indicates the inhalation and exhalation states in each breathing period. This breathing signal can be potentially used as the breathing signature for the identification of the subject's health conditions [1]. Fig. 6(d) shows the reference signal from the gas pressure sensor [14] in the chest belt and provides the ground truth for the breathing rate detected from our passive radar setup. As can be seen, there are still some differences compared to the chest belt result, but the results show high correlation.

Since the Doppler radar measuring rate is every 0.2 seconds abd the chest belt every 1.0 second, we use linear interpolation method to stretch belt signal so that it has the same length as micro Doppler signal. Based on the stretched belt signal and micro Doppler signal, we apply an FFT window to derive the dominant frequency of the breathing and plot the output in Fig. 7. Then pick the maximum absolute value of the output as the frequency that corresponds to the breath rate. As can be seen, both measured peak and belt peak are at about 0.2 Hz which gives 12.7 breaths/min. This result can be further improved by using a better scale resolution (longer FFT window). Also note that we use an FFT window of 30 seconds only. This window is long enough to capture the periodicity of breathing rate but short enough to react to an increase/decrease in breathing rate. The FFT is computed by overlapping windows that are shifted every 0.2s, hence providing a new estimate every 0.2s.

C. Experiment 1: Accuracy Versus Distance

We also validated system's ability to monitor a subject's breathing at different distances from surveillance antenna. In this experiment, the system layout is same as shown in Fig. 5. The subject sits on a chair at marked locations whose distances range from 0.2m to 1.0m away from the surveillance antenna respectively and breathes normally. In each experiment, the subject wears a chest belt and faces towards

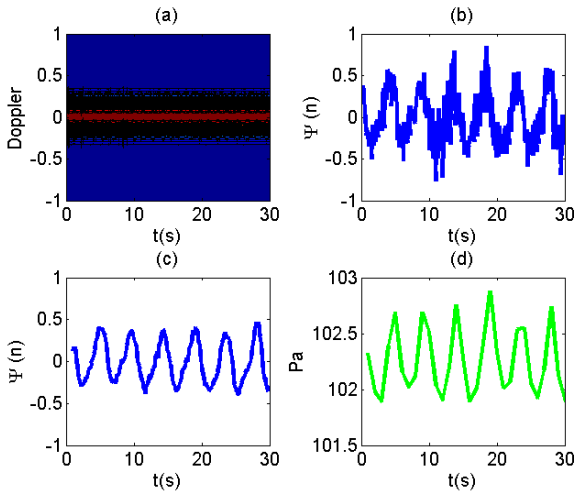

Fig. 6. Breathing signal from Doppler radar and chest belt, a) spectrogram of the breathing motion, b) micro Doppler without SG filter, c) micro Doppler with SG filter and d) ground truth: chest belt signal. The Doppler radar measuring rate is every 0.2 second, the chest belt measuring rate is every 1 second

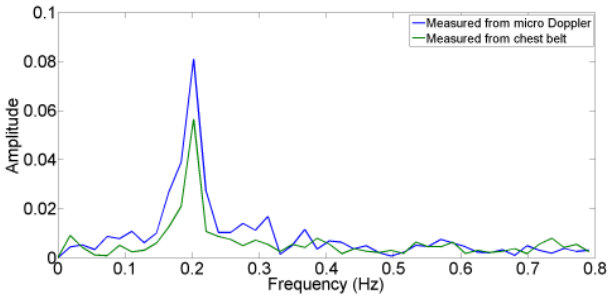

Fig. 7. Output of Fourier Transform for breathing rate measured by Doppler radar & chest belt

the surveillance antenna. We output the normalised micro Doppler from the passive system with normalised chest belt results simultaneously. Fig. 8 plots 30 seconds of normalized chest belt signal versus normalized micro Doppler signal at a) 20cm, b) 40cm, c) 60cm, d) 80cm, e) 100cm distance from surveillance antenna. To evaluate the accuracy of the micro Doppler output related to breathing rate, we perform an FFT of the signal in Fig. 8 and plot in Fig. 9. By picking the dominant frequency as breathing rate, the micro Doppler signal gives correct breathing rate in 20cm, 40cm, 60cm and 80cm scenarios at 0.2 Hz and has slightly incorrect in 100cm scenario at 0.21 Hz.

Based on the breathing signal shown in Fig. 8, we calculate mean-squared-error (MSE) and correlation-coefficient (Corr_Coeff) between micro Doppler and chest belt signals to demonstrate the accuracy of the system and shown in Table. I. As can be seen, MSE increases and Corr_Coeff decreases enormously when the distance is longer than 60cm. It can be visually observed from Fig. 8(d) and (e): low similarity between micro Doppler signal and chest belt signal. This drop in accuracy is because of the decreasing in signal-to-clutter-

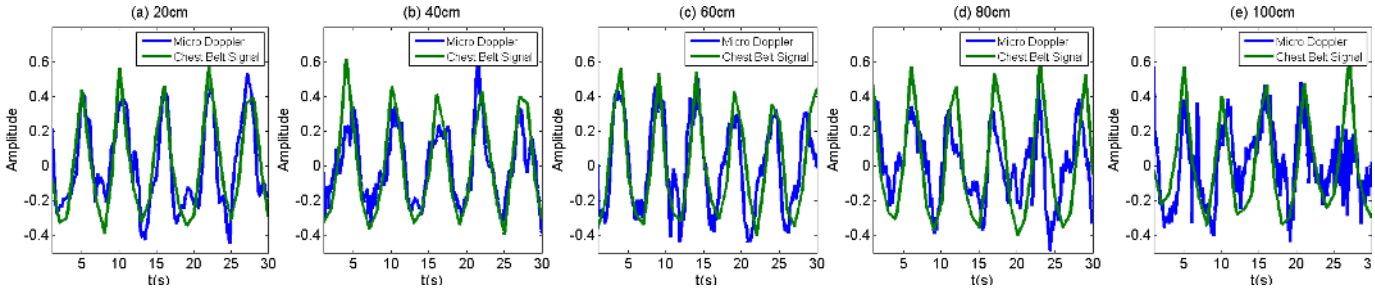

Fig. 8. Normalised chest belt signal versus normalized micro Doppler signal with a) 20cm, b) 40cm, c) 60cm, d) 80cm, e) 100cm distance from surveillance antenna. The Doppler radar measuring rate is every 0.2 second, the chest belt measuring rate is every at 1 second

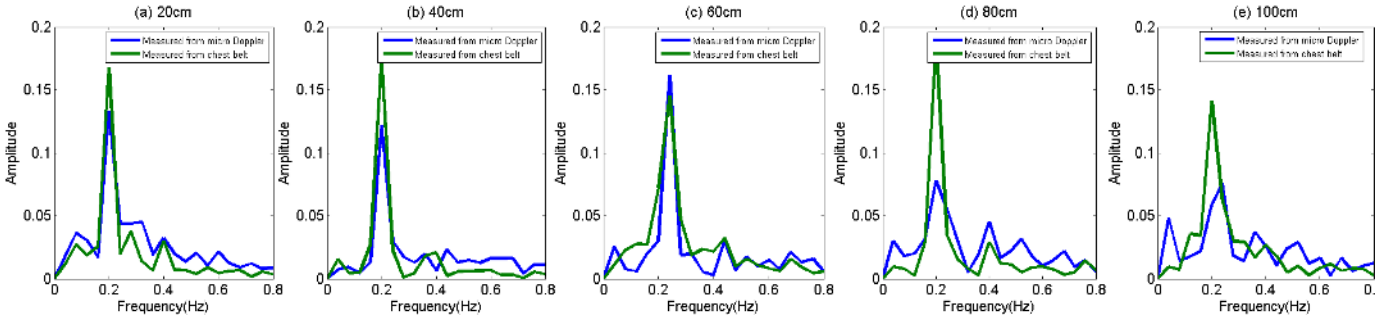

Fig. 9. Output of Fourier Transform for breathing rate measured by Doppler radar & chest belt with a) 20cm, b) 40cm, c) 60cm, d) 80cm, e) 100cm distance from surveillance antenna

ratio (SCR) which is the result of increased distance between subject and surveillance antenna.

TABLE I
EVALUATION OF DOPPLER RADAR MEASUREMENTS COMPARED TO CHEST BELT SIGNAL VERSUS DISTANCE

Distance	MSE	Corr_Coeff
20cm	0.1378	0.8532
40cm	0.1358	0.8583
60cm	0.1670	0.7935
80cm	0.2178	0.6432
100cm	0.2034	0.6022

D. Experiment 2: Accuracy Versus Orientations

In this experiment, we change the system layout to test the flexibility of the proposed system when deploying in real and practical situations. The EH transmitter is kept outside the experiment room while the subject and surveillance antennas remain in the same place as shown in Fig. 5 with distance of 40cm. There is a 20cm brick wall between the subject and EH source. The distance between the subject and the wall is 2m. The reference antenna is 1m away from the wall and pointing to the EH transmitter. The experiment layout is shown in Fig. 10. To further validate that the system operates correctly even when the subject does not face towards the antenna, the subject breathing is measured from different orientations: i) subject faces to the antenna, ii) subject faces right perpendicular to the antenna, iii) subject faces left perpendicular to the antenna and iv) subject back to the antenna.

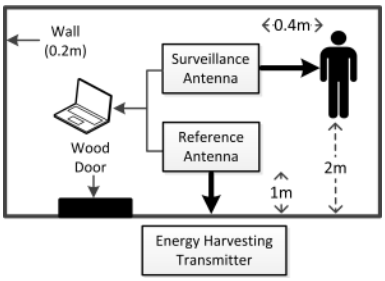

Fig. 10. Experiment layout: separated illuminator

The Fig. 11 plots the normalised chest belt signal versus normalised micro Doppler signal, Fig. 11(a) shows the face orientation, Fig. 11(b) shows the right orientation, Fig. 11(c) shows the left orientation and Fig. 11(d) shows the back orientation. Comparing with the reference chest belt signal, the corresponding micro Doppler records show clear periodical characteristics. These preliminary results clearly present that the passive system has the ability to detect the micro Doppler shift triggered by the subject's chest motion even the surveillance antenna is not facing subject's chest. This feature increases the flexibility of proposed non-contact system when deployed in loose controlled situation.

The Table. II shows MSE and Corr_Coeff of the normalised micro Doppler signal in comparison to the normalised chest belt signals. As can be seen, the face and back orientations give higher accuracy than right and left orientations. The reason is that chest movement is relatively small at two sides which

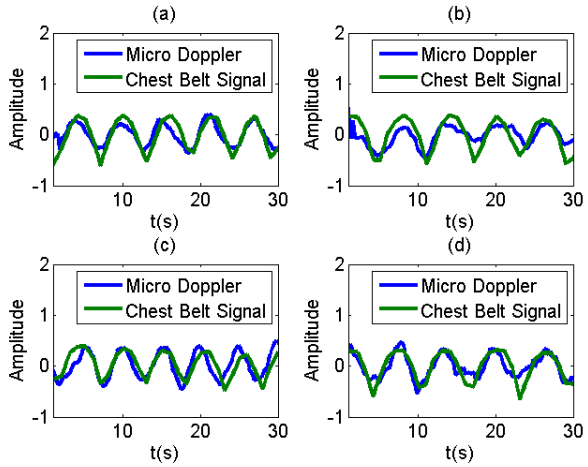

Fig. 11. Normalised chest belt signal versus normalised micro Doppler signal with four orientations to surveillance antenna. (a) face orientation, (b) right orientation, (c) left orientation, and (d) back orientation

results in less Doppler shift. Also we notice that the accuracy of face orientation (0.1542 & 0.8441) is similar to the same distance (40cm) in Experiment 1 (0.1358 & 0.8583) shown in Table. I. Both results illustrate the accuracy of proposed passive system is related to the distance between surveillance antenna and subject when using EH transmitter as illuminator within a short range. However, we need more data to verify the effective distance between EH transmitter to subject and surveillance antenna.

TABLE II
EVALUATION OF DOPPLER RADAR MEASUREMENTS COMPARED TO CHEST BELT SIGNAL VERSUS ORIENTATIONS

Orietations	MSE	Corr_Coeff
Face	0.1542	0.8441
Right	0.2048	0.7369
Left	0.1930	0.6928
Back	0.1688	0.7797

IV. CONCLUSION AND FUTURE WORK

In this paper, a novel non-contact breathing monitoring system has been presented. We have shown the feasibility of passive radar in capturing breathing rate with a low frequency and narrow-band signals. A novel micro Doppler extraction method is proposed to enable the passive system to measure breathing rate. This method can be also extended to other passive radar systems to detect the micro Doppler shifts. The human breathing have been conducted with distances from 20cm to 100cm away from the Doppler radar in a realistic environment. The results show that the passive system is able to capture the breathing signal accurately up to 60cm and breathing rate up to 100cm. The system has also been tested for difficult illumination conditions with four different orientations. The measured breathing signal has been compared with the chest belt result as the ground truth and shows high correlation.

Future work would be extended to involve heartbeat detection. Since our passive system uses low frequency and narrow-band signal, the heartbeat might be very challenging due to the even smaller Doppler shift and extra signal attention of the body tissue.

ACKNOWLEDGMENT

This work was performed under the SPHERE IRC funded by the UK Engineering and Physical Sciences Research Council (EPSRC), Grant EP/K031910/1.

REFERENCES

[1] Y. Lee, P. Pathirana, R. Evans, and C. Steinfort, "Noncontact detection and analysis of respiratory function using microwave doppler radar," in *Journal of Sensors*, 2015, p. 13.

[2] Respiration: Single or dual-band. [Online]. Available: http://vivonoetics.com/products/vivosense/analyzing/respiration-single-or-dual-band/

[3] P. Arlotto, M. Grimaldi, R. Naeck, and J.-M. Ginoux, "An ultrasonic contactless sensor for breathing monitoring," *Sensors*, vol. 14, 2014.

[4] R. Fletcher and J. Han, "Low-cost differential front-end for doppler radar vital sign monitoring," in *Microwave Symposium Digest, 2009. MTT '09. IEEE MTT-S International*, June 2009, pp. 1325–1328.

[5] L. Liu, Z. Liu, and B. Barrowes, "Through-wall bio-radiolocation with uwb impulse radar: Observation, simulation and signal extraction," *Selected Topics in Applied Earth Observations and Remote Sensing, IEEE Journal of*, vol. 4, no. 4, pp. 791–798, Dec 2011.

[6] A. Sharafi, M. Baboli, and M. Eshghi, "A new algorithm for detection motion rate based on energy in frequency domain using uwb signals," in *Bioinformatics and Biomedical Engineering (iCBBE), 2010 4th International Conference on*, June 2010, pp. 1–4.

[7] X. Li, D. Qiao, Y. Li, and H. Dai, "A novel through-wall respiration detection algorithm using uwb radar," in *Engineering in Medicine and Biology Society (EMBC), 2013 35th Annual International Conference of the IEEE*, July 2013, pp. 1013–1016.

[8] B. Tan, K. Woodbridge, and K. Chetty, "A real-time high resolution passive wifi doppler-radar and its applications," in *Radar Conference (Radar), 2014 International*, Oct 2014, pp. 1–6.

[9] M. C. Tang, F. K. Wang, and T. S. Horng, "Human gesture sensor using ambient wireless signals based on passive radar technology," in *Microwave Symposium (IMS), 2015 IEEE MTT-S International*, May 2015, pp. 1–4.

[10] C. Moscardini, D. Petri, A. Capria, M. Conti, M. Martorella, and F. Berizzi, "Batches algorithm for passive radar: a theoretical analysis," *Aerospace and Electronic Systems, IEEE Transactions on*, vol. 51, no. 2, pp. 1475–1487, April 2015.

[11] Y. Yang, N. Tong, C. Feng, and S. He, "Micro-doppler extraction of rotating targets based on doppler rate," in *Signal Processing, Communications and Computing (ICSPCC), 2011 IEEE International Conference on*, Sept 2011, pp. 1–4.

[12] Ni usrp 2920. [Online]. Available: http://sine.ni.com/nips/cds/view/p/lang/en/nid/212995

[13] O. Kaltiokallio, H. Yigitler, R. Jantti, and N. Patwari, "Non-invasive respiration rate monitoring using a single cots tx-rx pair," in *Information Processing in Sensor Networks, IPSN-14 Proceedings of the 13th International Symposium on*, April 2014, pp. 59–69.

[14] Vernier gas pressure sensor. [Online]. Available: http://www.inds.co.uk/education/sensors/gaspressure.htm